The Journal of Systems and Software 84 (2011) 923–929

Contents lists available at ScienceDirect

The Journal of Systems and Software

journal homepage: www.elsevier.com/locate/jss

A novel image watermarking in redistributed invariant wavelet domain

Li Li[a,*], He-Huan Xu[a], Chin-Chen Chang[b], Ying-Ying Ma[a]

[a] Institute of Computer Graphics and Image Processing, Hangzhou Dianzi University, 2nd Street, Xiasha, Hangzhou 310018, China
[b] Department of Information Engineering and Computer Science, Feng Chia University, Taichung 20724, Taiwan, ROC

ARTICLE INFO

Article history:
Received 16 September 2010
Received in revised form
21 December 2010
Accepted 10 January 2011
Available online 19 January 2011

Keywords:
Image watermarking
Haar wavelet
Copyright protection
Geometric attacks

ABSTRACT

Most existing digital watermarking algorithms, which are based on the Discrete Wavelet Transform, are not robust to geometric distortions, even if for some special distortions, such as multiples of 90° rotation of integers and image flipping, which change the location of pixels but have no effect on the value of the image. Therefore, to solve the problem, according to Haar wavelet transform theory, the redistributed invariant wavelet domain is constructed and proofed in this paper; a novel image watermarking algorithm, based on the invariant domain, is proposed to eliminate such distortions. The experimental results showed that the proposed algorithm not only can resist the common image processing operations, but also successfully resist the distortions that result from multiples of 90° rotations of integers and image flipping.

1. Introduction

The rapid development of information technologies has created an urgent demand for copyright protection of digital media, since it can be reproduced and manipulated in many convenient ways. Therefore, watermarking techniques were introduced to solve these problems, and these techniques have been studied extensively.

Image watermarking, which is a powerful technique for protecting the copyright of images, slightly modifies the host digital images to embed the copyright information. Currently, many researchers are committed to this filed and lots of new methods are continually proposed. Chang et al. (2009) presented a novel removable watermarking algorithm utilizing the Just Noticeable Distortion (JND) technique and the correlation difference between two selected subsampling images. Wang et al. (2010) proposed a steganographic scheme to improve the hiding capacity of EMD method (Zhang and Wang, 2006). Huang and Fang (2010) discussed about the practical implementation of robust watermarking with the EXIF metadata.

According to the processing domain in which the watermark is embedded, image watermarking techniques can be divided into two categories, i.e., spatial domain (Schyndel et al., 1994; Bender et al., 1996) and frequency domain (Cox et al., 1997; Bami et al., 1998; Premaratne and Ko, 1999; Xie and Arce, 2001). Generally speaking, frequency domain watermarking schemes are more robust to tampering and attacks than those in spatial domain. The discrete cosine transform (DCT), discrete Fourier transform (DFT) and discrete wavelet transform (DWT) domains are three common frequency domains that are commonly used in most image watermarking schemes. In addition, watermarking in DWT domain has drawn extensive attention for its good time-frequency features and its accurate matching of the human visual system (HVS).

For a watermarking system to be successful, the watermark must resist a variety of possible attacks. Usually, attacks on a watermarking scheme can be classified as common image processing operations and geometric distortions (Zheng et al., 2007). Although most existing watermarking schemes based on DWT have been demonstrated to be effective against common image processing, it is still inadequate in facing the challenge of resisting geometric distortions. This is because the DWT coefficients are not invariant under geometric transforms. For example, rotating an image by 90°, 180°, or 270° will not affect the value of the image, but any of the three rotations may lead to failure in detecting the watermark.

There are three procedures that are used in existing watermarking methods to address the issue of geometric distortions (Gao et al., 2010). The first procedure is to embed a template along with the watermark as side information. Pereira and Pun (2000) proposed a method based on the use of a template in the DFT domain. Before the detection of the watermark, the affine geometric attacks in the image were estimated and corrected by the embedded template. A major problem is that the template-based methods are incapable of estimating the attack parameters for some complicated geometric attacks.

* Corresponding author. Tel.: +86 13666632945; fax: +86 0571 86871632.
E-mail addresses: lili2008@hdu.edu.cn, lilihzdz@gmail.com (L. Li), xhhjin@gmail.com (H.-H. Xu), ccc@cs.ccu.edu.tw (C.-C. Chang), m7051986@163.com (Y.-Y. Ma).

0164-1212/$ – see front matter © 2011 Elsevier Inc. All rights reserved.
doi:10.1016/j.jss.2011.01.025

The second procedure is to use feature-based watermarking techniques. Bas et al. (2002) utilized the Harris detector to extract the feature points. Then, they defined a number of triangular regions, and both the watermark embedding and detection were conducted in these triangles. The problem with such watermarking techniques is the excessive computational burden incurred in the detection due to the use of a robust descriptor (Xiang et al., 2008).

In the third procedure, the watermark is embedded into the geometric invariant domain. In Ruanaidh and Pun (1998), Lin et al. (2001) and Farzam and Shirani (2001), the researchers embedded the watermark in an invariant domain, such as the Fourier–Mellin transform or Zernike moments, as opposed to using affine transforms. However, watermarking schemes that involve an invariant domain are usually difficult to implement.

The introduction above demonstrates that it is still an open problem to deal with geometric attacks. In addition, considering the widespread use of DWT in image watermarking techniques, it would be useful to determine ways to enhance the robustness of wavelet-based image watermarking schemes against geometric distortions.

In this paper, an invariant wavelet domain is constructed and proved, and, then, based on this proven invariant wavelet domain, a novel watermarking technique is proposed. Obviously, our method belongs to the third procedure that embeds the watermark in the geometric invariant domain, and it is quite easy to accomplish. In order to achieve geometric invariance, first, the pixels' locations of the image are redistributed; then, the Haar wavelet transform and some normalized procedures are performed, and, finally, the invariant wavelet domain is obtained. As we have proved in detail in Section 3.2, it is robust to some geometric distortions, such as multiples of 90° rotation of integers and image flipping, which change the positions of the pixels of the image but leave their values unchanged. Consequently, most existing wavelet-based watermarking schemes, blind or not blind, can be redesigned by using the invariant wavelet domain to enhance their robustness to cope with geometric distortions. Experimental results show that the proposed scheme is really robust to geometric attacks, and, more importantly, it is still able to resist common image processing.

The rest of this paper is organized as follows. A brief review of the Haar wavelet transform is given in Section 2. In Section 3, the proposed redistributed invariant wavelet domain is constructed and proved. Section 4 details the novel image watermarking scheme in two subsections, i.e., embedding and detection. Experimental results and analysis are presented in Section 5, and Section 6 concludes this work.

2. Haar wavelet transform

Recently, wavelet-based watermarking schemes have begun to attract greatly increased attention. The main reasons for inserting watermarks in the wavelet domain are that it has good space-frequency localization, superior HVS modeling, and low computational cost. In practice, when a watermark is to be embedded in the wavelet domain, there are many wavelet bases to choose from. Since the different bases have different characteristics, the choice of which base to use to embed the watermark is important. In their research, Liu et al. (2003) found that the Haar wavelet is suitable for watermarking images.

Let $I(x, y)$ denote a digital image of size $2M \times 2N$, if not, boundary prolongation should be used to ensure that the size of the image is divisiable by 2, which is necessary for Haar wavelet transform. The wavelet low-pass and high-pass filters are $h(n)$ and $g(n)$ respectively. Then the image can be decomposed into its various resolutions based on the approximate weight (LL) and the detailed

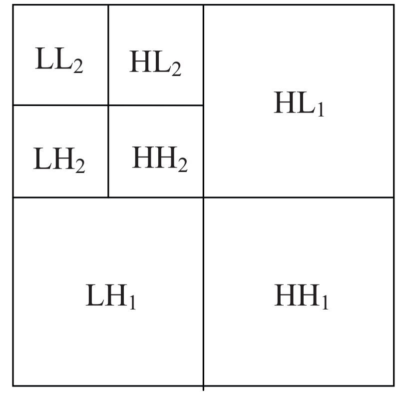

Fig. 1. Two-level wavelet decomposed image.

weights of the horizontal direction (HL), vertical direction (LH), and diagonal direction (HH). The decomposition formula is:

$$\begin{cases} LL(i,j) = \sum_{x,y} h(x-2i)h(y-2j)I(x,y), \\ LH(i,j) = \sum_{x,y} h(x-2i)g(y-2j)I(x,y), \\ HL(i,j) = \sum_{x,y} g(x-2i)h(y-2j)I(x,y), \\ HH(i,j) = \sum_{x,y} g(x-2i)g(y-2j)I(x,y), \end{cases} \tag{1}$$

where $i, j, N \in Z^+$, $x, y \in Z$, $-2L+1 \le x-2i \le 0$, $-2L+1 \le y-2i \le 0$.

On this basis, similar decomposition procedure can be implemented on LL to get the two-level wavelet transformed image, as shown in Fig. 1, and so on. The wavelet image reconstruction is the inverse transform of the wavelet decomposition. The formula is:

$$I(x,y) = \sum_{i,j} h(x-2i)h(y-2j)LL(i,j) + \sum_{i,j} h(x-2i)g(y-2j)LH(i,j) + \sum_{i,j} g(x-2i)h(y-2j)HL(i,j) + \sum_{i,j} g(x-2i)g(y-2j)HH(i,j), \tag{2}$$

where $i, j, N \in Z^+$, $x, y \in Z$, $-2N+1 \le x-2i \le 0$, $-2N+1 \le y-2i \le 0$.

As for the Haar wavelet, the low-pass filter is $\{1/\sqrt{2}, 1/\sqrt{2}\}$, and the high-pass filter is $\{1/\sqrt{2}, -1/\sqrt{2}\}$, so Formula (1) can be rewritten as Formula (3):

$$\begin{cases} I_{LL}(i,j) = [I(2i-1,2j-1) + I(2i-1,2j) + I(2i,2j-1) + I(2i,2j)]/2, \\ I_{LH}(i,j) = [I(2i-1,2j-1) - I(2i-1,2j) + I(2i,2j-1) - I(2i,2j)]/2, \\ I_{HL}(i,j) = [I(2i-1,2j-1) + I(2i-1,2j) - I(2i,2j-1) - I(2i,2j)]/2, \\ I_{HH}(i,j) = [I(2i-1,2j-1) - I(2i-1,2j) - I(2i,2j-1) + I(2i,2j)]/2, \end{cases} \tag{3}$$

where $1 \le i \le M$, $1 \le j \le N$.

3. Our redistributed invariant wavelet domain

In this section, the construction and proof procedures of the redistributed invariant wavelet domain are described in detail in Sections 3.1 and 3.2, respectively.

3.1. Construction of redistributed invariant wavelet domain

For the purpose of invariance to multiples of 90° rotation and image flipping, given an image I, the normalization procedure is formulated as follows:

Step 1: Divide the original image into four (2×2), equal-sized subimages and derive their average intensities matrix, denoted as:

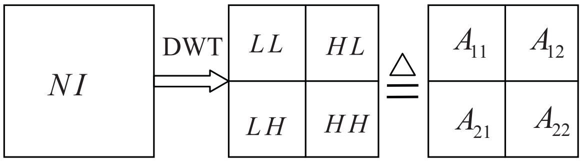

Fig. 2. One-level decomposed matrix of the redistributed image.

$\text{mean} = \begin{pmatrix} a & c \\ b & d \end{pmatrix}$, $a, b, c, d \geq 0$.

Step 2: Define the Normalization Matrix S as:

$$S \triangleq \begin{pmatrix} S_{11} & S_{12} \\ S_{21} & S_{22} \end{pmatrix} = \begin{pmatrix} a+b+c+d & a+b-c-d \\ a-b+c-d & a-b-c+d \end{pmatrix}.$$

Meanwhile, assume that S_{11}, S_{12}, S_{21}, S_{22} are all unequal to zero and that $|S_{21}| \neq |S_{12}|$. (For a natural image, it usually meets the conditions.) Then, extract the Sign Matrix, denoted by:

$$Sign = \begin{pmatrix} Sg_{11} & Sg_{12} \\ Sg_{21} & Sg_{22} \end{pmatrix}, \quad Sg_{ij} \in \{-1, +1\}.$$

Step 3: Redistribute the original image, and note the new, redistributed image as *NI*. In this way, the redistributed rule between the original image and redistributed image can be prescribed as Formula (4).

$$\begin{cases} NI(2i-1, 2j-1) = I(i, j) & 1 \leq i \leq M, 1 \leq j \leq N, \\ NI(2i-1, 2j-2N) = I(i, 3N-j+1) & 1 \leq i \leq M, N < j \leq 2N, \\ NI(2i-2M, 2j-1) = I(3M-i+1, j) & M < i \leq 2M, 1 \leq j \leq N, \\ NI(2i-2M, 2j-2N) = I(3M-i+1, 3N-j+1) & M < i \leq 2M, N < j \leq 2N. \end{cases} \quad (4)$$

Then, decompose the new image *NI* by one level, using the Haar wavelet transform, as can be seen in Fig. 2.

Step 4: Multiply the sub-band of the transformed image by the Sign Matrix, as shown in Fig. 3, and denote the matrix obtained as: $B = \begin{pmatrix} B_{11} & B_{12} \\ B_{21} & B_{22} \end{pmatrix}$.

Step 5: Matrix B is just the invariant wavelet domain if $|S_{21}| < |S_{12}|$. The term $|*|$ is the absolute value operator. Otherwise, swap B_{12} with B_{21} and transpose each sub-band of B to get a refreshed matrix B, that is $B = \begin{pmatrix} B_{11}^T & B_{21}^T \\ B_{12}^T & B_{22}^T \end{pmatrix}$, where B_{ij}^T denotes the transpose matrix of B_{ij}.

The final matrix B is the invariant wavelet domain; it is invariant to multiples of 90° rotation and image flipping. That is, once the original is flipped or rotated by multiples of 90°, the same wavelet domain can be achieved by above procedures.

3.2. Proof of redistributed invariant wavelet domain

To prove that the final matrix B is an invariant domain, we have rewritten the decomposition formula utilizing Formulas (3) and (4) for the redistributed image, and the result is Formula (5).

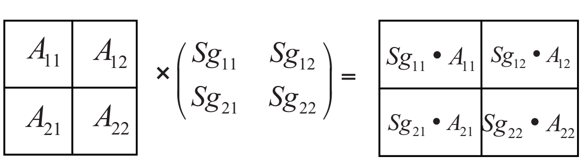

Fig. 3. Multiply the transformed image with the Sign Matrix.

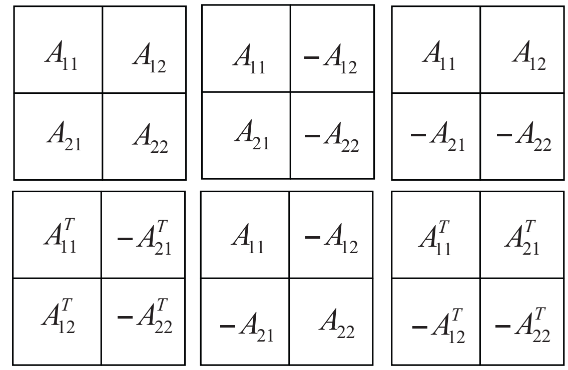

Fig. 4. Transformed matrices of attacked images decomposed by Formula (5): (a) original image, (b) horizontal flipping, (c) vertical flipping, (d) 90° rotating, (e) 180° rotating, and (f) 270° rotating.

$$\begin{cases} NI_{LL}(i, j) = [I(i, j) + I(i, 2N+1-j) + I(2M+1-i, j) + I(2M+1-i, 2N+1-j)]/2, \\ NI_{LH}(i, j) = [I(i, j) - I(i, 2N+1-j) + I(2M+1-i, j) - I(2M+1-i, 2N+1-j)]/2, \\ NI_{HL}(i, j) = [I(i, j) + I(i, 2N+1-j) - I(2M+1-i, j) - I(2M+1-i, 2N+1-j)]/2, \\ NI_{HH}(i, j) = [I(i, j) - I(i, 2N+1-j) - I(2M+1-i, j) + I(2M+1-i, 2N+1-j)]/2, \end{cases} \quad (5)$$

where $1 \leq i \leq M$, $1 \leq j \leq N$.

To decompose an original image by Formula (5), denote the transformed matrix as A. Rotating or flipping the image afterwards, it is not difficult to find that the transformed matrix (by Formula (5)) of the attacked image is related to matrix A, as shown in Fig. 4. Observe the following: (1) the change in the transformed matrix is fixed for a definite geometric distortion; (2) the transpose of matrix A_{ij} and the swap of A_{12} and A_{21} always occur simultaneously.

Therefore, there are only two problems that must be solved to achieve an invariant domain, i.e., one is the sign change, and the other is the matrix transpose. First, to eliminate the sign effect, we divide the original image into four (2 × 2), equal-sized sub-images and derive their average intensities matrix; then, we obtain the Normalization Matrix and Sign Matrix, and, last, by multiplying the sub-bands of the transformed image by the corresponding signs of the Sign Matrix, we can get the refreshed matrices without the sign problem. Second, in order to conquer the matrix transpose, we define a normalized process, i.e., if $|S_{21}| < |S_{12}|$, leave the transformed matrix B untouched; otherwise, swap B_{12} with B_{21} and transpose each sub-band of B to get a redefined matrix B.

In this case, the final matrix B will be robust to some geometric attacks, such as image flipping and multiples of 90° rotations, and it is just the redistributed invariant wavelet domain.

4. Novel watermarking scheme based on invariant wavelet domain

Most existing digital watermarking algorithms based on the wavelet domain are sensitive to geometric distortion, since the wavelet coefficients are not invariant under geometric attack. In this paper, by constructing a redistributed invariant wavelet domain, we proposed a novel algorithm for redesigning many wavelet-based, image-watermarking schemes to resist geometric attacks.

To demonstrate the use of redistributed invariant wavelet domain, take the additive embedding as an example. By inserting the watermark in the low sub-band (LL_2) of the two-level decomposed image, we give the embedding and detection algorithms as follows.

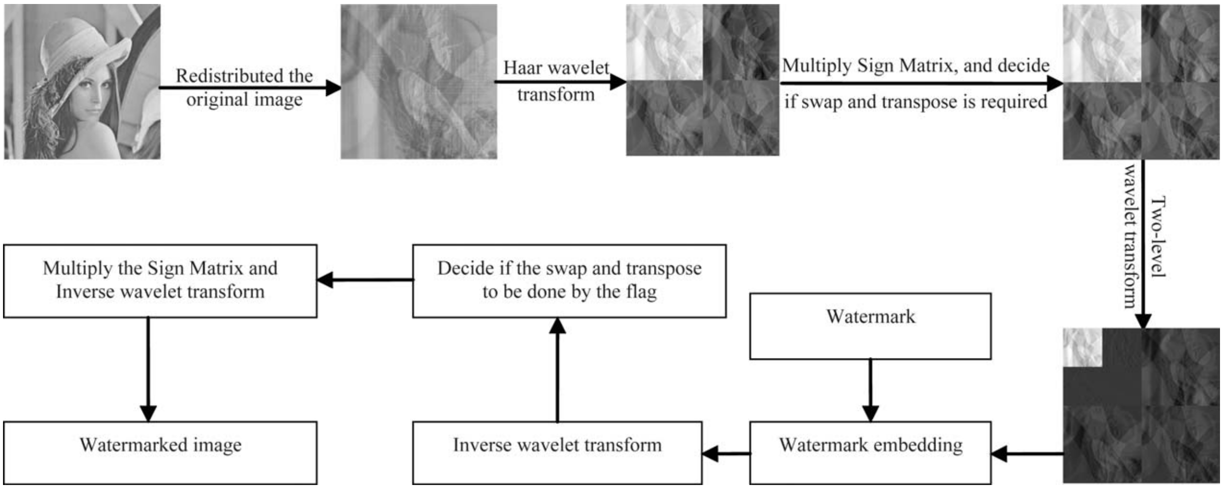

Fig. 5. Flowchart of watermark embedding.

4.1. Watermark embedding

To embed a watermark into a given image, we first obtain its redistributed invariant wavelet domain B by the method described in Section 3.1; at the same time, we make a flag at Step 5 to record if a swap and transpose are necessary or not; afterwards, we decompose the low sub-band of B, i.e., B_{11}, using DWT and the derived, four sub-bands as LL_2, LH_2, HL_2 and HH_2; finally, we embed the watermark into LL_2 with the following formula:

$$F'(u, v) = F(u, v) + \alpha W_i. \tag{6}$$

where $F(u, v)$ is the wavelet coefficients, α is the scaling factor, and W_i is the watermark. As for a scaling factor, α is used to control the watermark embedding strength. If α has greater value, the robustness is better and the watermarked image quality is worse; Instead, if α has smaller value, the watermarked image quality is better and the robustness is worse. In practice, α is chosen differently according to different applications.

To get the watermarked image, first, we perform an inverse wavelet transform to get a modified matrix of B; then, we have to decide if a swap and transpose are required by the flag and do it; next, we multiply the sub-band of modified matrix B by the Sign Matrix and derive a modified matrix of A; last, we use the Haar inverse wavelet transform to obtain the final watermarked image. Fig. 5 shows the flowchart of watermark embedding.

4.2. Watermark detection

In this algorithm, both the original image and the watermark W are needed, and the detector determines only whether or not a given watermark has been embedded in the detecting image. The steps for watermark detection are as follows:

(1) Both the original and the detecting images are processed to get the invariant wavelet domains as described in Section 3.1;
(2) The low sub-bands (LL) of invariant wavelet domains are decomposed again by DWT.
(3) By comparing the two-level low sub-band (LL_2) of the original and detecting images, a watermark W^* is detected.
(4) Compute the similarity $\rho(W^*, W)$ between W^* and the watermark W as:

$$\rho(W^*, W) = \frac{\sum_i w_i^* \cdot w_i}{\sqrt{\sum_i (w_i^*)^2}}. \tag{7}$$

(5) If $\rho(W^*, W)$ is greater than a threshold T, then indicate that the watermark is detected; otherwise, indicate that it is absent.

The detection process is shown in Fig. 6.

5. Experimental results and analysis

We use a 256×256, grayscale Lena image as the original test image, and the watermark consists of a sequence of real numbers with a length of 4096, with each number chosen independently according to the normal distribution $N(0,1)$. The algorithms and attacks are all performed in a MATLAB 7.6 environment, and the Haar wavelet is used to compute the DWT. Peak Signal-to-Noise Ratio (PSNR) is used to measure the quality of the watermarked or attacked images.

Setting the detection threshold is a classical decision estimation problem. Here, it is pre-determined as six, and, in this way, if W^* is created independently from W, then the probability that $\rho(W^*, W) > 6$ is the probability of a normally distributed random variable exceeding its mean by more than six standard deviations.

We illustrate and evaluate the performance of the original and proposed schemes based on their imperceptibility and robustness. Table 1 shows the PSNR value and the watermark similarity under different strength of the scaling factor. It can be seen that, as the scaling factor improves, the PSNR value between the watermarked and original image decreases; at the same time, the similarity between the detected and original watermark increases. In addition, their performances are very similar, i.e., they will have a similar perceptual quality.

Table 1
The PSNR and similarity under different scaling factors.

Scaling factor	PSNR (dB)		Similarity	
	Original	Proposed	Original	Proposed
5	45.2071	45.2071	62.9592	62.9592
6	43.5895	43.6264	63.5190	63.5190
7	42.4042	42.4042	63.7996	63.7996
8	41.2795	41.2795	63.9796	63.9796
9	40.2938	40.2938	64.1207	64.1207
10	39.4256	39.4256	64.2274	64.2274
11	38.6167	38.6531	64.2857	64.2857
12	37.8928	37.8928	64.3418	64.3418
13	37.2049	37.2412	64.3918	64.3918
14	36.6265	36.6265	64.4269	64.4269
15	36.0409	36.0409	64.4460	64.4460

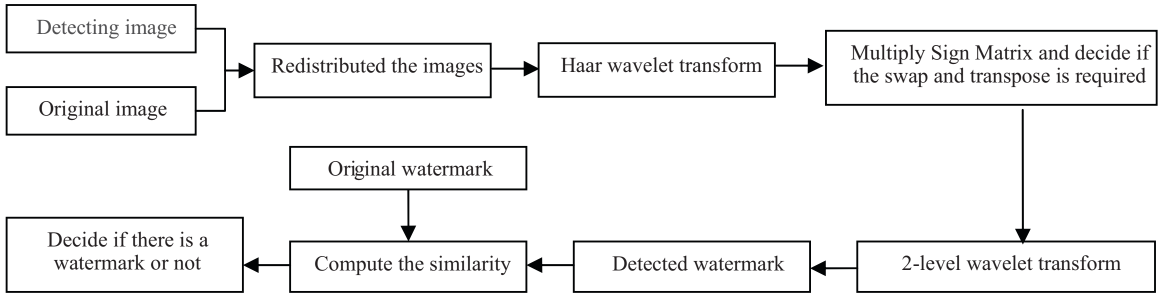

Fig. 6. Flowchart of watermark detection.

Fig. 7. Watermarked images: (a) watermarked image by original scheme and (b) watermarked image by proposed scheme.

Table 2
The watermark similarity (geometric distortions).

Attack type	Similarity	
	Original	Proposed
No attack	63.9796	63.9796
Rotating 90°	−0.8029	63.9796
Rotating180°	0.2779	63.9796
Rotating 270°	0.1318	63.9796
Horizontal flipping	−0.4437	63.9796
Vertical flipping	−1.3343	63.9796

To evaluate the robustness of the original and proposed schemes, we fix the scaling on eight, and the watermarked images are shown in Fig. 7; meanwhile, the comparison between their histograms and the histograms of the original image is demonstrated in Fig. 8. It is clear that no perceptual degradation can be found in the two watermark images, and the histogram analyses also indicate that their histograms are similar.

Then, some common image processing operations and geometric distortions are conducted, i.e., rotation, flipping, adding noise, and JPEG compression, as shown in Fig. 9. Table 2 shows the watermark similarity of the two schemes; Tables 3 and 4 present the related PSNR and the similarity values under Gaussian noise and JPEG compression, respectively.

It can be observed from Table 2 that the proposed scheme has a better performance against geometric attacks, i.e., when the watermarked image is rotated or flipped, the original scheme will not work, while the same high similarity can be detected by the proposed scheme. For common image processing operations, Tables 3 and 4 show that the proposed scheme has a very similar performance, in most cases, with the original method, and maybe the similarity value of the proposed scheme is slightly lower than the original scheme in JPEG compression, but even the PSNR is lowered to 27.0296 dB the similarity (11.9628) is still far beyond the threshold of 6, which will not affect the detection of the watermark.

Accordingly, when coping with common image processing operations, both of the schemes show a similar perceptual quality and

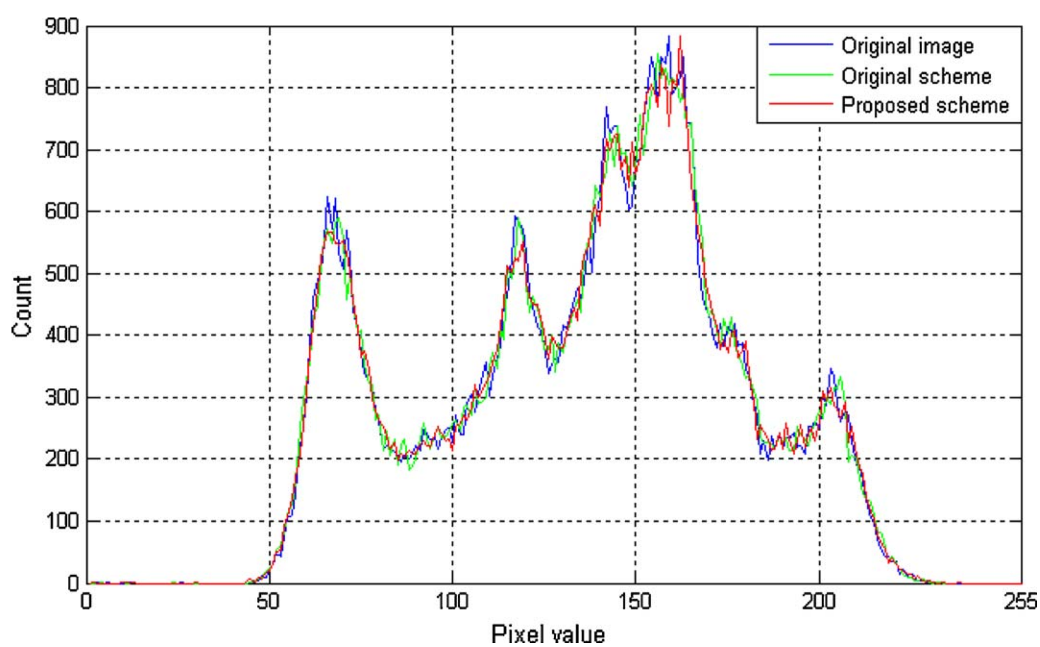

Fig. 8. Histogram analyses of Lena for original and proposed schemes.

Fig. 9. Attacked images: (a) original image, (b) rotating 90°, (c) rotating 180°, (d) rotating 270°, (e) horizontal flipping, (f) vertical flipping, (g) Gaussian noise (the parameter is 0.01), and (h) JPEG compression (the quality factor is 10).

Table 3
The PSNR and similarity (adding Gaussian noise).

Parameter ($\times 10^{-2}$)	PSNR (dB)		Similarity	
	Original	Proposed	Original	Proposed
0.1	28.9033	28.8936	45.3444	45.8735
0.2	26.0119	25.9956	35.9558	38.3330
0.3	24.3405	24.3333	32.3431	33.0102
0.4	23.0929	23.0999	30.3072	29.5378
0.5	22.1066	22.1036	25.2133	26.2676
0.6	21.3519	21.3426	23.4644	25.5327
0.7	20.6814	20.6859	23.1357	22.1806
0.8	20.1040	20.1042	21.9040	21.7603
0.9	19.6310	19.6325	19.9152	19.0211
1.0	19.2049	19.2043	19.8477	19.4734

Table 4
The PSNR and similarity (JPEG compression).

Quality factor	PSNR (dB)		Similarity	
	Original	Proposed	Original	Proposed
10	26.9645	27.0296	19.6596	11.9582
20	28.8897	28.9817	38.1457	26.0473
30	29.9213	30.0270	47.6863	35.4101
40	30.6923	30.8152	52.7715	41.6776
50	31.3602	31.4573	55.7860	46.7360
60	32.0479	32.1267	57.8516	51.0780
70	32.9850	33.0726	60.3516	55.1599
80	34.3830	34.4774	62.1708	59.1119
90	36.8080	36.8596	63.4134	62.2458

robustness; however, once the watermarked image is attacked by geometric transform, such as 90° multiples of integer rotation and image flipping, the original scheme fails completely, but the proposed scheme still works well.

Hence, most existing, wavelet-based image watermarking schemes, like those presented in Kundur and Hatzinakos (1998) and Xia et al. (1998), could be redesigned by the proposed redistributed invariant wavelet domain that is robust to geometric distortions.

6. Conclusions

In this paper, a redistributed invariant wavelet domain is proposed and proved; it is resistant to multiples of 90° rotations and image flipping. On this basis, a novel redesigned method for most wavelet-based watermarking algorithms is presented. Experimental results show that the redesigned method is really robust to some geometric attacks, and at the same time, it does not damage the performance of the original scheme. Therefore, the proposed scheme is more robust than the related watermarking schemes.

Acknowledgements

This work is partially supported by the National Natural Science Foundation of China (No. 60703087), the Project of Science and Technology Department of Zhejiang Province (No. 2008C13080, No. 2010C31006). The authors also gratefully acknowledge the helpful comments and suggestions of the reviewers, which have improved the presentation.

References

Bami, M., Bartolini, F., Cappellini, B., Piva, A., 1998. A DCT domain system for robust image watermarking. Signal Processing 66 (3), 357–372.
Bas, P., Chassery, J.M., Macq, B., 2002. Geometrically invariant watermarking using feature points. IEEE Transactions on Image Processing 11 (9), 1014–1028.
Bender, W., Gruhl, D., Morimoto, N., Lu, A., 1996. Techniques for data hiding. IBM System Journal 35 (3&4), 313–336.
Chang, C.C., Lin, P.Y., Yeh, J.S., 2009. Preserving robustness and removability for digital watermarks using subsampling and difference correlation. Information Sciences 179 (13), 2283–2293.
Cox, I.J., Kilian, J., Leighton, F.T., Shamoon, T., 1997. Secure spread spectrum watermarking for multimedia. IEEE Transactions on Image Processing 6 (12), 1673–1687.
Farzam, M., Shirani, S., 2001. A robust multimedia watermarking technique using Zernike transform. In: Proceedings of 2001 IEEE Fourth Workshop on Multimedia Signal Processing , Cannes, France, pp. 529–534.
Gao, X., Deng, C., Li, X., Tao, D., 2010. Geometric distortion insensitive image watermarking in affine covariant regions. IEEE Transactions on Systems, Man, and Cybernetics 40 (3), 278–286.
Huang, H.C., Fang, W.C., 2010. Metadata-based image watermarking for copyright protection. Simulation Modelling Practice and Theory 18 (4), 436–445.
Kundur, D., Hatzinakos, D., 1998. Digital watermarking using multiresolution wavelet decomposition. In: Proceedings of the 1998 IEEE International Conference on Acoustics, Speech, and Signal Processing , Seattle, WA, USA, pp. 2969–2972.
Lin, C.Y., Wu, M., Bloom, A., Cox, I.J., Miller, M.L., Lui, Y.M., 2001. Rotation, scale, and translation resilient public watermarking for images. IEEE Transactions on Image Processing 10 (5), 767–782.
Liu, J.F., Huang, D.R., Hu, J.Q., 2003. The orthogonal wavelet bases for digital watermarking. Journal of Electronics & Information Technology 25 (4), 453–459.
Pereira, S., Pun, T., 2000. Robust template matching for affine resistant image watermarks. IEEE Transactions on Image Processing 9 (6), 1123–1129.

Premaratne, P., Ko, C.C., 1999. A novel watermark embedding and detection scheme for images in DFT domain. In: Proceedings of Seventh International Conference on Image Processing and its Applications, vol. 2 , Manchester, UK, pp. 780–783.
Ruanaidh, J., Pun, T., 1998. Rotation, scale and translation invariant spread spectrum digital image watermarking. Signal Processing 66 (3), 303–317.
Schyndel, R.G.V., Tirkel, A.Z., Osborne, C.F., 1994. A digital watermark. In: Proceedings of IEEE International Conference on Image Processing, vol. 2 , Austin, TX, USA, pp. 86–90.
Wang, Z.H., Kieu, T.D., Chang, C.C., Li, M.C., 2010. A novel information concealing method based on exploiting modification direction. Journal of Information Hiding and Multimedia Signal Processing 1 (1), 1–9.
Xia, X.G., Boncelet, C.G., Arce, G.R., 1998. Wavelet transform based watermark for digital images. Optics Express 3 (12), 497–511.
Xiang, S., Kim, H.J., Huang, J., 2008. Invariant image watermarking based on statistical features in the low-frequency domain. IEEE Transactions on Circuits and Systems for Video Technology 18 (6), 777–790.
Xie, L.H., Arce, G.R., 2001. A class of authentication digital watermarks for secures multimedia communication. IEEE Transactions on Image Processing 10 (11), 1754–1764.
Zhang, X., Wang, S., 2006. Efficient steganographic embedding by exploiting modification direction. IEEE Communications Letters 10 (11), 1–3.
Zheng, D., Liu, Y., Zhao, J.Y., Saddik, A.E., 2007. A survey of RST invariant image watermarking algorithms. ACM Computing Surveys 39 (2), 1–91.

Li Li, Received Ph.D from Zhejiang University in 2004. She research on images/video/mesh watermarking and image processing. She research on Image and 3D mesh watermarking Algorithms as Research Assistant In Hong Kong Polytechnic University form 2002.11–2003.5. She has published more than 60 papers.

He-Huan Xu, postgraduate student of Hangzhou Dianzi University. He research on image watermarking and image processing.

Chin-Chen Chang, Professor Chin-Chen Chang obtained his Ph.D. degree in computer engineering from National Chiao Tung University. His first degree is Bachelor of Science in Applied Mathematics and master degree is Master of Science in computer and decision sciences. Both were awarded in National Tsing Hua University. Dr. Chang served in National Chung Cheng University from 1989 to 2005. His current title is Chair Professor in Department of Information Engineering and Computer Science, Feng Chia University, from Feb. 2005. Professor Chang's specialties include, but not limited to, data engineering, database systems, computer cryptography and information security. He has published more than 1000 Papers. For more infomation (http://www.myiecs.iecs.fcu.edu.tw/_visitor/teacher/teacher_pro.php?fdno=T93142).

Ying-Ying Ma, postgraduate student of Hangzhou Dianzi University, She research on image watermarking and image processing.